CHAPTER-6

6.1.Introduction

In present chapter, Sr-Ti mixed metal oxide is emphasized as a heterogeneous base catalyst in transesterification reaction for methyl ester production from WCO. The most efficient active phase of catalyst was explored by varying the Sr/Ti atomic ratio in mixed metals oxide. The synthesized catalyst underwent for TGA/DSC, Powder XRD, SEM, EDX, FT-IR, XPS, and BET surface area analysis to assess its physicochemical characteristics. Additionally, basicity, the most process governing factor was also evaluated through Hammett indicator-benzoic acid titration method. The Sr-Ti mixed metals oxide with 4:1 was observed with highest catalytic activity for methanolysis reaction. Its potency was facilitated by fairly acquired BET surface area ($43.6 m^2/g$) and basic strength (2.89mmol/g). The appreciable values of both the parameters imparted the high catalytic activity in Sr-Ti mixed metals oxide with atomic ratio 4:1. Onward, transesterification reaction was optimized for the maximum FAME conversion through RSM using CCD. The confirmatory tests showed the consistency with conclusions drawn from RSM study regarding the optimized values of concerned process variables. Transesterification reaction turned out with 98.15±0.75% FAME conversion exerting catalyst dose (1.0 wt %), methanol to oil molar ratio (11:1), and reaction time (80 min) at reaction temperature (65˚C) and agitation speed (600rpm) featured by RSM study. The closeness in optimized value of anticipated and confirmatory results perceived the efficiency of CCD and approving its potency as successful tool to estimate the reaction process for highest methyl ester conversion. Next, a pseudo-first-order kinetic model was established on transesterification reaction having activation energy (E_a) of

29.67kJ/mol. In addition to this, thermodynamic functions were also computed through Eyring plot dictating the non-spontaneity and endergonic nature of transesterification reaction. The Environment-factor (E-factor) and turn over frequency (TOF) were enumerated and they approved the prepared Sr-Ti mixed metals oxide as an efficient and sustainable catalyst for the production of methyl esters through transesterification. Finally, all the important fuel properties of prepared methyl esters from waste cooking oil was discerned within the range laid by ASTM D-6751 standards which coined the compatibility of prepared methyl ester with CI engines as a substitute of diesel fuel.

6.2. Catalyst synthesis

Sr-Ti mixed metal oxides with Sr/Ti atomic ratio (1:2, 1:1, 2:1, 3:1, 4:1, and 5:1) were synthesized by polymer precursor method. The stipulated amount of strontium nitrate was dissolved in the saturated aqueous solution. This aqueous solution of strontium nitrate was added to the ultrasonicated aqueous solution of TiO_2 (stoichiometrically taken to maintain the above mentioned atomic ratios with Sr). An equimolar aqueous solution of citric acid was appended as a complexing agent to both Sr and Ti, with continuous agitation at 600 rpm on hot plate at 65˚C. Afterwards, Nitrate-citrate salt was made unlikely to be unstable by putting 25% ammonia solution into reaction mixture unless pH 7 was achieved. Afterwards, resulted sol was allowed to stir vigorously at 120˚C to form gel. Onward complete gelation, entire reaction mixture was auto combusted at 350˚C. The extensive firing of reaction mixture at this temperature triggered the evolution of volatile carbonaceous products and nitrate degradation changing the color of dry gel to grey. This way the crude Sr/Ti mixed metal oxide catalyst was prepared. Later, the crude catalyst underwent for thermal analysis which predicted the calcination temperature at 880 ˚C in muffle furnace for the

optimized time interval of 8h with heating rate of 10˚C/min. Finally, the calcined catalyst was applied in transesterification after grinding with agate pestle and mortar.

6.3. Design of experiments

Transesterification experiments were systematically devised by RSM using CCD via MINITAB 16. Three independent process variables (catalyst dose; X_1, methanol to oil molar ratio; X_2, and reaction time; X_3) were accounted in optimization process designed by CCD to analyze the effect of operation condition on FAME conversion. RSM consists of various statistical and mathematical methodologies to optimize the response which generally depends upon numbers of independent variables (Razack and Duraiarasan, 2016). RSM is quite prominent method to explore the impact of an individual factor over response. Furthermore, the interactive effect of process variables can also be found out using RSM (Sahani et al., 2019b). It overpowers the classical method where effects of process variable taken into account one after other which is too time consuming. Moreover, a classical method does not provide any information regarding the interaction of any two parameters quantitatively. RSM does overcome this issue by giving the access of various designs to seek the possible effect of interactions among parameters on response. RSM study furnishes out the pictorial results i.e. surface and contour plots, representing the response manipulated by considered process variables. The range of individual parameter was decided through the preliminary experiments done to explore the highest FAME conversion and depicted in the Table 6.1. Here, CCD has incorporated above three process parameters with five degrees of freedom ($-\alpha$, -1, 0, $+1$, $+\alpha$) furnishing total 20 experiment illustrated in Table 6.2.

Table 6.1

Level of variables chosen for CCD in FAME conversion during base catalysed transesterification reaction

Factors		**Coded values**		
		+1	0	-1
Catalyst dose (wt%)	χ_1	05	1.05	1.8
Oil to methanol molar ratio	χ_2	1:3	13	1:23
Reaction time (min)	χ_4	20	70	120

Table 6.2

An illustration of experimental runs formulated by central composite design for biodiesel production with 6 center points and α value of 1.68179.

Standard order	**Run order**	**Pt types**	**Blocks**	**Catalyst dose**	**Methanol to oil molar ratio**	**Time**	**FAME conversion**
20	1	0	1	1.00000	10.0000	60.000	92
18	2	0	1	1.00000	10.0000	60.000	93
14	3	-1	1	1.00000	10.0000	110.4	75
4	4	1	1	1.50000	15.0000	30.000	19
3	5	1	1	0.50000	15.0000	30.000	35
19	6	0	1	1.00000	10.0000	60.000	92
12	7	-1	1	1.00000	18.4090	60.000	35
1	8	1	1	0.50000	5.0000	30.000	51
13	9	-1	1	1.00000	10.0000	9.546	36
10	10	-1	1	1.84090	10.0000	60.000	59
6	11	1	1	1.50000	5.0000	90.000	49
8	12	1	1	1.50000	15.0000	90.000	75
17	13	0	1	1.00000	10.0000	60.000	91
7	14	1	1	0.50000	15.0000	90.000	53
9	15	-1	1	0.15910	10.0000	60.000	44
16	16	0	1	1.00000	10.0000	60.000	93
2	17	1	1	1.50000	5.0000	30.000	35
5	18	1	1	0.50000	5.0000	90.000	56
11	19	-1	1	1.00000	1.5910	60.000	10
15	20	0	1	1.00000	10.0000	60.000	88

A plausible correlation between response i.e. FAME conversion and independent variables could be demonstrated by mathematical expression which is second order polynomial equation here. Here, +α and−α denote the minimum and maximum coded axial values framed by CCD in this RSM study.

$$Y = \beta_0 + \sum_i^3 \beta_i X_i + \sum\sum_{i<j=1}^3 \beta_{ij} X_i X_j + \sum_i^3 \beta_{ii} X_i^2 \quad (6.1)$$

Where Y is the predicted response (FAME conversion), and X_i and X_j are coded independent process variables. β_0, β_i, β_{ii}, and β_{ij} are the model constant, linear effect, quadratic effect and interaction effect predicted by RSM.

6.3.1. Catalyst characterization

6.3.2. Thermal analysis

The uncalcined catalyst was thermally treated to check the impact of temperature over its mass. TGA/DSC plot figured out the three consequent mass disintegrations occurred at 35-215˚C, 220-425˚C, and 433-850˚C with 14.2%, 22.4%, and 18.8% mass losses respectively. All three degradation processes were not sharply defined as in Figure 6.1 reflected by TGA/DSC plots. In fact, each mass loss event occurred over a wide temperature range as no sharp peak regarding heat flow was obtained in DSC. Nevertheless, the first mass loss step happened at 35˚C-215˚C as also arisen in DSC attributing to an endothermic process of dehydration of catalyst surface and its lattice (Yadav et al., 2018). The major second weight loss of about 22.4% happened at 220-425˚C assigned by an exothermic peak in DSC owing to degradation of nitrates from precursors and organic residues from reaction mixture (Roy et al., 2019). Next mass disintegration belonged to an exothermic process of CO and CO_2 desorption due to the combustion of residual organic matter which eventuated in the

temperature range of 433-880˚C with 18.8% mass loss (Sahani and Sharma, 2019). After 880˚C, there was no considerable mass loss in TGA plot which ascertained the same temperature as calcination temperature. All the catalyst samples with different Sr/Ti atomic ratio were calcined at 880˚C.

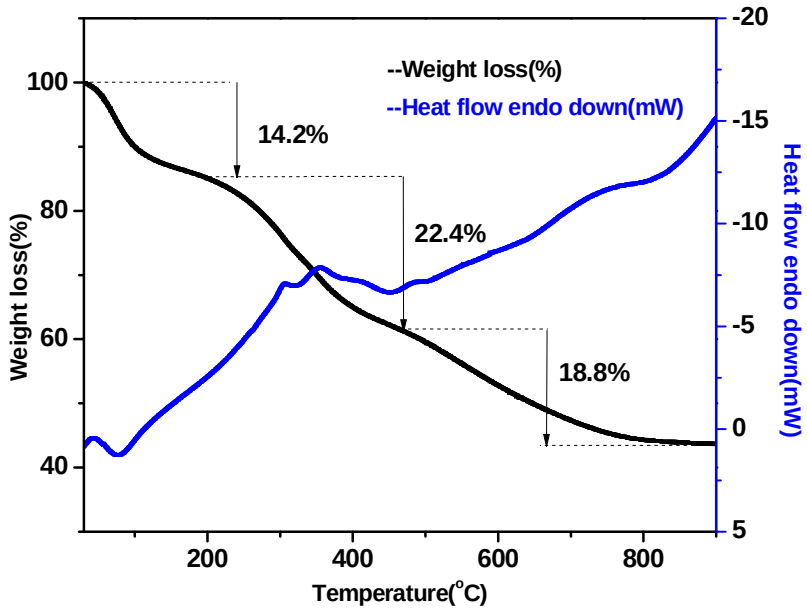

Figure 6.1 TGA–DTA of crude Sr-Ti mixed metals oxide as solid catalyst.

6.3.3. Powder XRD analysis

X-ray diffraction analysis was done to identify the crystallite phase, cell parameters and also the lattice arrangement of synthesized catalyst. Figure 6.2 reveals diffractogram of calcined catlysts with different Sr/Ti atomic ratio (1:2, 1:1, 2:1, 3:1, 4:1, and 5:1). The prominent peaks appeared in diffractogram were assigned with respective phase structure according to the JCPDS database. Sr/Ti with 1:2 incorporated two phases i.e. $SrTiO_3$ and TiO_2 as peaks regarding $SrTiO_3$ (placed at 2θ values of 22.7˚(100), 32.4˚(110), 39.9˚(111), 46.5˚(200), 52.3˚(210), 57.8˚(211), 67.8˚(220), 77.2˚(310), 81.7˚(311), and 86.2˚(222) reported in JCPDS file no. 894934)

and TiO_2 (positioned at 27.31˚(110), 35.86˚(110), 39.1˚(200), 40.98˚(111), 54.02˚(211), 56.37˚(220), and 63.71˚(310) detailed in JCPDS file no. 896975) appeared in Figure 6.2. Sr/Ti ratio with 2:1 has got Sr_2TiO_4 as prominent peaks corresponding the same has been noticed at 2θ values of 23.91˚(101), 31.35˚ (103), 32.56˚ (110), 43.05˚(006), 46.73˚(200), 55.03˚ (116), 57.33˚ (213), 65.41˚ (206), and 68.21˚ (220) also appeared in JCPDS file no. 391471.

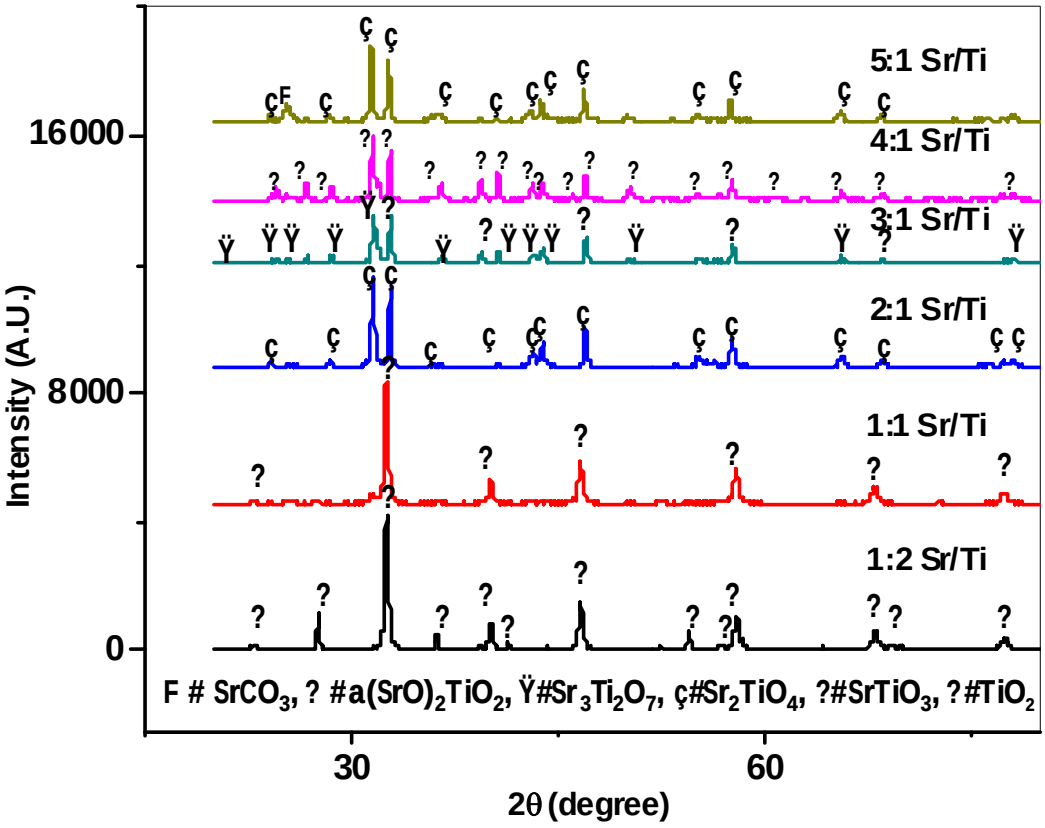

Figure 6.2 X-Ray diffractogram of prepared Sr-Ti mixed metal oxide with different atomic ratio (1:2,1:1,2:1,3:1,4:1,and 5:1).

Sr/Ti with 3:1 received two coexisting phase structures of $Sr_3Ti_2O_7$ and $SrTiO_3$, the former manifested its presence through the prominent peaks at 26.96˚ (101), 30.61˚ (006), 36.87˚ (105), 37.92˚ (110), 49.95˚ (116), 52.10˚ (00$\underline{10}$), 54.64˚ (200), 66.23˚ (11$\underline{10}$), and 67.95˚ (215) congruent with respective peaks in JCPDS file no.782479. Sr/

Ti ratio with 4:1 has come up with $(\alpha\text{-SrO})_2TiO_2$ formula by reflecting the high intensity peaks at 23.95˚ (101), 28.30˚(004), 31.34˚(103), 32.57˚(110), 43.03˚(006), 46.73˚(200), 55.00˚(116), 57.35˚(213), 65.41˚ (206), 68.24˚ (220) found coincident with the peaks in JCPDS file no. 722041. Sr/Ti ratio has assimilated two of existing phases i.e. Sr_2TiO_4 and $SrCO_3$; former one depicted its appearance at 2θ values of 23.92˚(101), 31.29˚(103), 32.53˚(110), 43.10˚(006), 46.69˚(200), 55.10˚ (116), 57.29˚ (213), 65.37˚ (206), and 68.19˚ (220) while the noticeable peaks addressing to the latter phase resided at 25.19˚(111) and 44.12˚(132)(JCPDS file no.712393). Due to presence of the $SrCO_3$ catalyst lost its basicity to an extent resulting in reduction in basic active sites for methanolysis (Sahani et al., 2019).

6.3.4. Surface morphological analysis

The surface morphology of catalyst samples with different metal stoichiometric ratio was investigated through SEM analysis. Figure 6.3 represents SEM image of all the calcined Sr-Ti metal oxides (with Sr/Ti 1:2, 1:1 2:1, 2:1 , 3:1 , 4:1 , and 5:1). It can be perspicuously observed that Sr/Ti with 1:2 has mixture of two different phases of $SrTiO_3$ and TiO_2 accompanying cylindrical and spherical shaped particles. Next, particles in catalyst samples (with Sr/Ti 1:1 2:1, 2:1 , 3:1 , 4:1, and 5:1) are composed of native oxides of both Sr and Ti i.e. SrO and TiO_2. The particles regarding these samples are shaped spherically as in Figure 6.3(b, c, d, e, & f). As the doping level of Sr increases the particle clearly turned into exclusively well assorted spherical shape but this trend was followed till catalyst sample with Sr/Ti 4:1. Beyond that owing to strong philicity of Sr, $SrCO_3$ was started forming and became indispensable in lattice of catalyst which was also reported by X-Ray diffractogram in Figure 6.3 and FT-IR spectra in Figure 6.5. This could also easily seen in Figure 6.3(f) for case of atomic

ratio 5:1 as carbonate species got irreversibly attached to the mixed metal oxide lattice and causing it to agglomerate with abruptly bigger size. Even it has not been removed at that much higher temperature of 880˚C. This might has caused contamination of basic active sites present on catalyst surface (Lima et al., 2012).

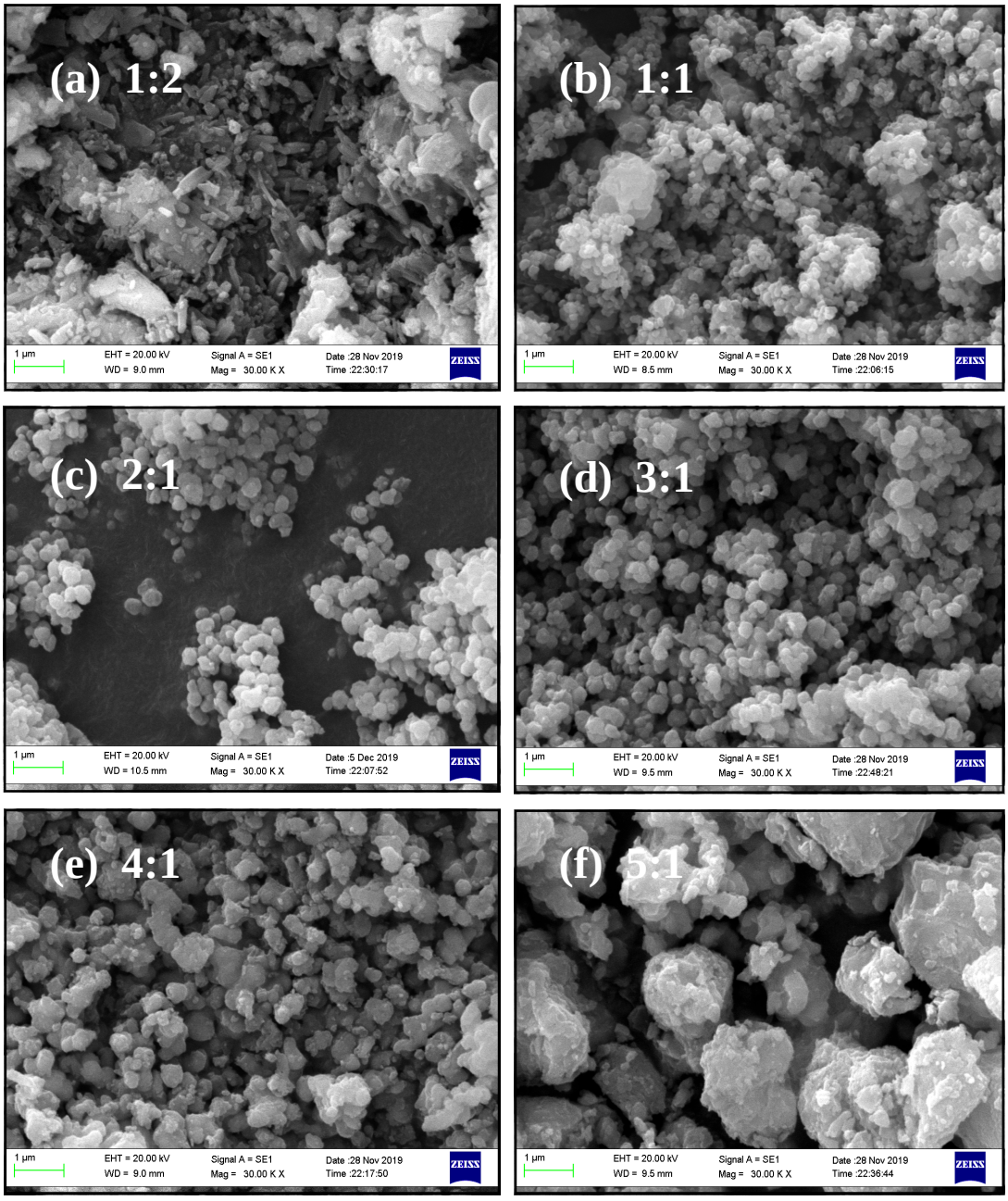

Figure 6.3 SEM images of prepared Sr-Ti mixed metal oxide with different atomic ratio (1:2, 1:1, 2:1, 3:1, 4:1, and 5:1).

This catalytic poisoning has declared the catalyst with Sr/Ti atomic ratio 5:1 catalytically inactive for FAME production through methanolysis in current study. Hence, catalyst with Sr-Ti with 4:1 has got the highest number of basic sites free of carbonate poisoning. Later the elemental analysis (EDXS) of Sr-Ti mixed metals oxide reported the weight% and atomic % of elements present in catalyst described in Figure 6.4(a). The particle size distribution of prepared catalyst with Sr/Ti atomic ratio 4:1 was derived from SEM image in Figure 6.3(e) using Image-J software as in Figure 6.4(b). The average particle size of the catalyst was found to be 350nm.

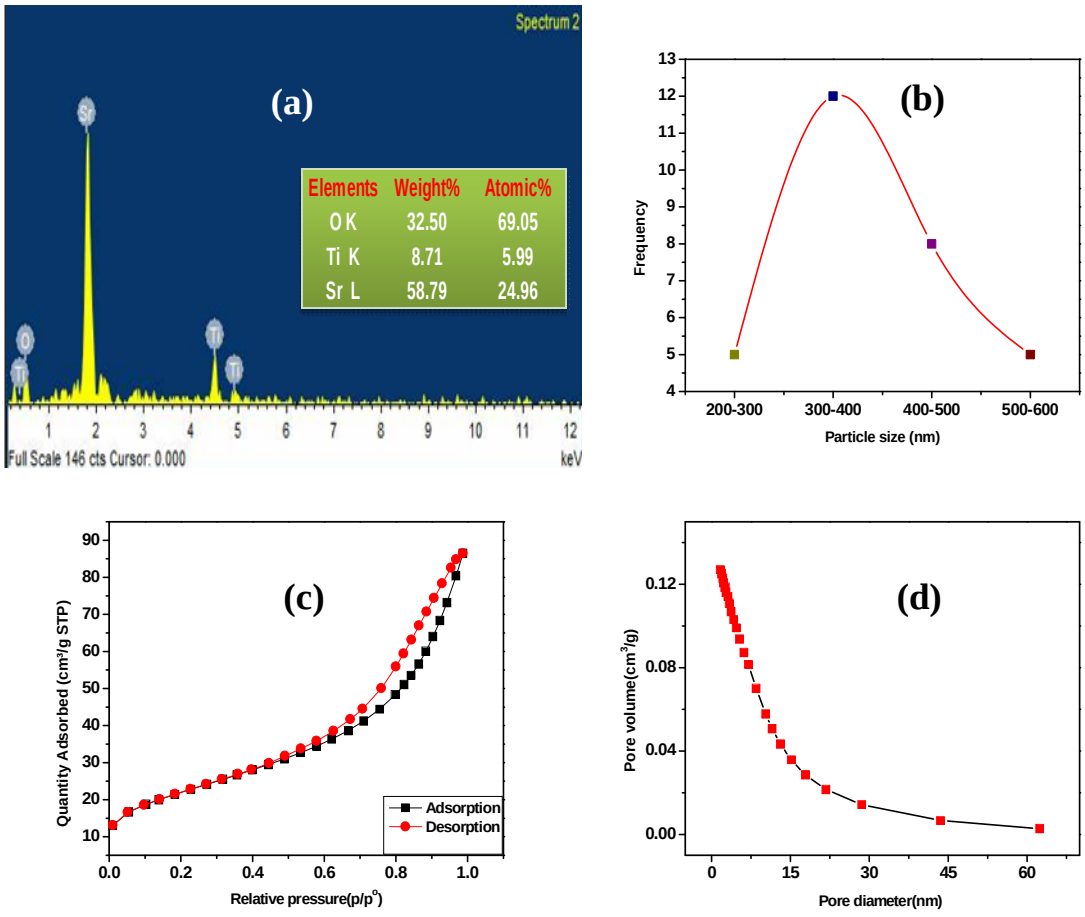

Figure 6.4 (a) EDX spectra**,** (b) particle size distribution inferred from SEM micrograph,(c) N_2 adsorption-desorption profile of the catalyst; (d) BJH adsorption pore size distribution of the catalyst.

6.3.5. FT-IR analysis

FT-IR analysis observed all the existing functional groups attached on surface of catalyst responsible for methyl ester conversion. Figure 6.5 represents the FT-IR spectra of calcined samples with different Sr/Ti ratio (1:2, 1:1, 2:1, 3:1, 4:1, and 5:1) at 880˚C. The broad band present in spectra of each catalyst samples around 3438 cm^{-1} revealed the O–H stretching vibration of chemisorbed moisture entrapped in KBr pellet formation required for FT-IR analysis (Singh et al., 2016). The high intensity peak arouse at 612 cm^{-1} were associated to octahedron Ti-O stretching vibration in catalyst samples (Ghamsari and Bahramian, 2008). The major difference in sample with Sr/Ti 5:1 was the appearance of peak at 1442 cm^{-1} in Figure 6.5 interpreted as C-O vibration due to the extreme philicity of alkaline Sr metal with carbonate appeared even

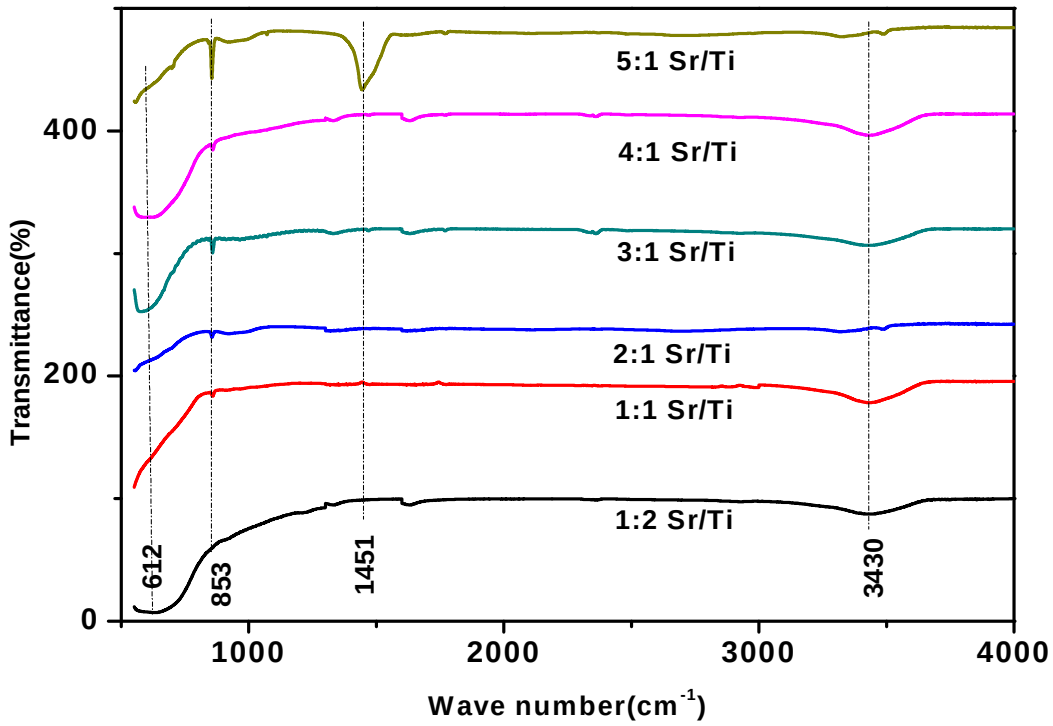

Figure 6.5 FT-IR spectra of prepared catalyst calcined at different temperature.

after calcination at 880 °C (Singh et al., 2016; Boschini et al., 2003). The appearance of $SrCO_3$ has been also substantiated by XRD analysis (Figure 6.2). This might be the sole reason for meager catalytic performance of Sr/Ti atomic ratio of 5:1 which was ultimately reflected through experiments of methanolysis.

6.3.6. XPS analysis

The detailed description of oxidation state of elements in Sr-Ti mixed metal oxides was extracted by X-ray photoelectron spectroscopy (XPS) analysis. X-Ray Photoelectron spectrum of Sr-Ti mixed metal oxide was illustrated in Figure 6.6 consisting elements individual spectra alongwith their wide scan. Figure 6.6(a) depicts core level spectra of Sr 3d present in mixed metal oxide of Sr-Ti. The X-Ray Photoelectron spectra of Sr 3d has a broad experimental peak which was further split into two characteristic peaks i.e. Sr $3d_{3/2}$ and Sr $3d_{5/2}$ due to spin orbit coupling appeared at 134.2 eV and 132.7 eV with FWHM values of 2.4eV and 2.6 eV, respectively. The exclusive position of signal attributing to Sr $3d_{5/2}$ has asserted the presence of Sr^{+2} in catalyst in form of SrO substantiating the inference of XRD which had indicated the structural formula of catalyst $(SrO)_2TiO_2$ (Dupin et al., 2000). Figure 6.6(b) consists two well separated maxima placed at 463.4 eV and 458.2 eV regarding Ti $2p_{1/2}$ and $2p_{3/2}$ generated due to spin orbit coupling with FWHM of 3.2 eV and 2.35 eV, successively. The positions of above two peaks affirmed the Ti^{4+} as TiO_2 in the bulk mixed metal oxide vindicating the results of XRD above (Xu et al., 2016). O1s core level spectra in Figure 6.6(c) has only one distorted peak excited by AlK_α radiation which was further fit into two peaks observed at 529.2 eV with FWHM of 1.8 eV and the other at 531.6 eV associated with FWHM of 2.9eV. The peak at relatively lower binding energy was correlated to oxygen specie physically adsorbed hydroxyl species on the surface of catalyst while peak with

higher binding energy was due to bulk oxygen present in lattice of catalyst as mixed metals oxide (Pilleux et al., 2014). Figure 6.6(d) constituted the wide scan X-Ray Photoelectron spectra displaying the residence of Sr, Ti, and O elements in synthesized catalyst.

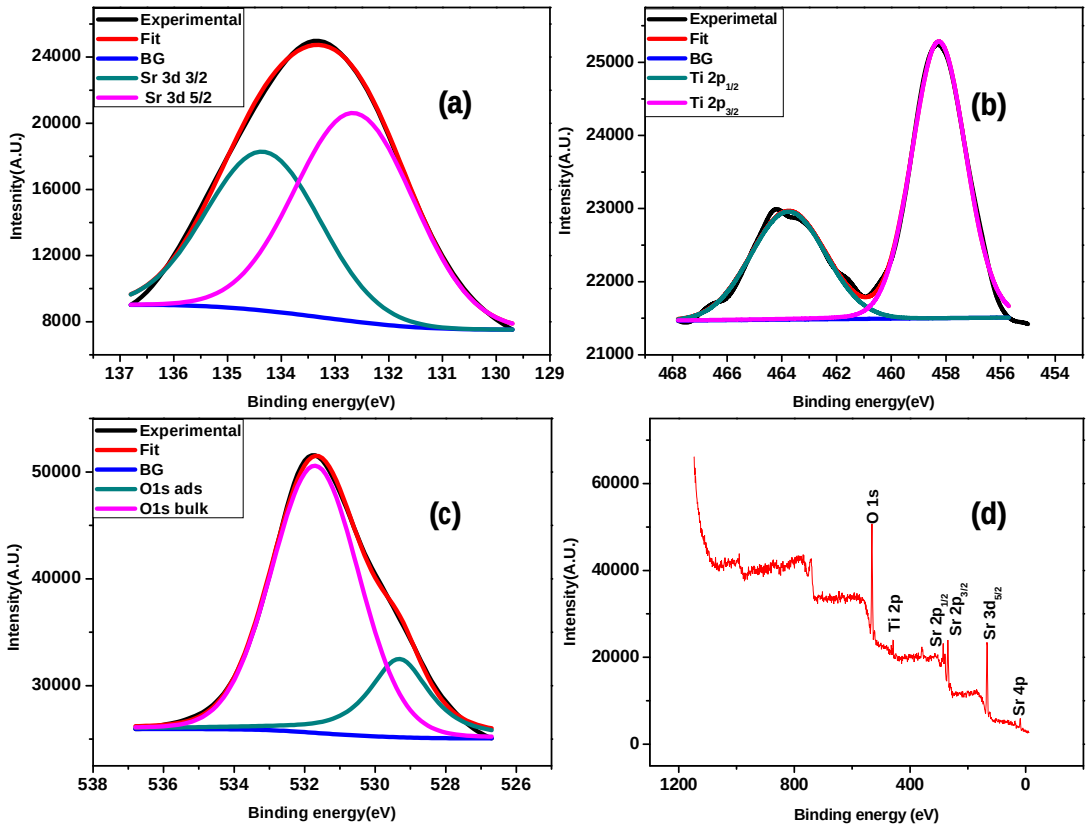

Figure 6.6 X-Ray Photoelectron spectra of catalyst i.e. Sr-Ti mixed metal oxide with atomic ratio (4:1)(a) Sr 3d spectra,(b) Ti 2p spectra,(c) O 1s spectra (d) wide scan full spectrum of catalyst.

6.3.7. BET surface area analysis

Surface area of catalyst plays a major role in any surface phenomena especially catalysis. But here in methanolysis, amount of surface area and basicity both together affect the FAME production. Nonetheless, basicity is more dominating factor than

surface area as the key process of transesterification is generation of acyl acceptor, i.e. methoxide ion on the surface of catalyst (Banerjee et al., 2019). This process is hastened by the strength of Lewis basicity of active sites present in catalyst. The available surface area for the methanolysis reaction over surface of the catalyst was tentatively quantified by Brunner, Emmett, Teller (BET) surface area analysis through N_2 adsorption-desorption isotherm linear plot illustrated in Figure 6.4(c). Additionally pore diameter and pore volume were also evaluated using the Barrett-Joyner-Halenda (BJH) method. Although the meso-porosity of synthesized catalyst which was found later most catalytically active, was insured by isotherm of typical type IV in Figure 6.4(d) with hysteresis loop which is a specific criterion of mesoporous solids (Sahani et al., 2019). S_{BET} of the most efficient catalyst i.e. Sr-Ti mixed metal oxide with atomic ratio (4:1) was quantified to be 43.6 m^2/g which was fair enough to carry out the transesterification reaction. Interestingly, the pore diameter or pore size was calculated and found to be 8.7125nm which was within 2-50 nm indicating the mesoporous structure of catalyst. This eased the diffusion of triglyceride (with size of 6 nm) due to size compatibility which accelerated the reaction as triglyceride diffused through pore swiftly and got closer to acyl acceptor and acyl moiety during chemical step of the entire reaction mechanism (Lee et al., 2014).

6.3.8. Basicity

Basicity is very decisive factor which decides the fate of methanolysis reaction by governing strength of catalyst (Sharma et al., 2009). Hammett indicator-benzoic acid titration method was employed for basic strength determination of catalyst. Lewis basic sites participate in neutralization process of benzoic acid during titration. The catalysts having high basic strength are always advantageous as in solid base catalysed

transesterification reaction, the cleavage of O-H bond is the key process of entire methanolysis reaction. Here, all catalyst samples with different Sr-Ti atomic ratio had undergone for acid-base titration using Hammett indicator method. The basicity of the catalyst was quantified by Hammett indicators with pk_a 6.8 < H_o or H_> 18.4 (neutral red, nile Red, bromthymol blue, phenolphthalein, 2,4-dinitroaniline, and 4-nitroaniline). The basic strength of synthesized catalyst samples are mentioned in Table 6.3. The basicity value of the Sr/Ti mixed metal oxide catalyst as a function of various atomic ratios 1:1, 2:1, 3:1, 4:1 and 5:1 calcined at 880˚C was assessed and interestingly their basic strength was obtained in increasing order with increase in Sr doing till 4:1 right from 1:2. The basicity of atomic ratio of Sr/Ti with 1:2 and 5:1 was found in the range of 6.8 (neutral Red) < H_< 10.2 (bromothymol blue) and average basic value was evaluated as 0.76 mmol/g and 0.83 mmol/g respectively. The exceptionally low value of basicity in case of 2:1 atomic ratio owed to the presence of carbonate species which drastically suppressed the theoretical increase in basicity due to increased Sr loading in catalyst i.e. 5:1. Additionally, it also added some acidic sites to catalyst surface. The relatively lower value of basic strength of catalyst with Sr/Ti 1:2 in comparison to others was Lewis acid sites present on surface of catalyst due to Ti^{4+} ion as Ti^{4+} O_2 has got feeble but somewhat acidic nature to carry out esterification of residual free fatty acids in waste cooking oil. There was further increment in basic value onward atomic rations 1:1 to 4:1 unless carbonate started entrapping in the lattice of catalyst. The atomic ration of 4:1 has acquired the highest basic number of sites with values 2.89 mmol/g falling in the range between 15.0 (2,4-dinitroaniline)<H_<18.4 (4-nitroaniline) respectively. This might be prime reason for the highest activity of Sr-Ti mixed metal oxide with atomic ratio 4:1 whereas other atomic ratios were discarded due to their

comparative incompatibility in transesterification reaction.

Table 6.3

BET surface area reports of Sr-Ti mixed metal oxides

Catalyst	Surface area (m^2/g)	Pore volume(cm^3/g)	Pore diameter(nm)
1:2 Sr/Ti	15.2	0.0297	6.1000
1:1 Sr/Ti	40.6	0.0617	7.3305
2:1 Sr/Ti	38.5	0.0698	8.1255
3:1 Sr/Ti	37.1	0.0785	8.0586
4:1 Sr/Ti	36.5	0.0811	7.5244
5:1 Sr/Ti	33.1	0.0432	2.3897

6.4. Optimization of transesterification reaction

6.4.1. Selection of efficient catalyst

Optimization of best Sr/Ti atomic ratio was performed by executing transesterification reaction with each of catalyst samples with Sr/Ti atomic ratio (1:2, 1:1, 2:1, 3:1, 4:1, and 5:1) by choosing the random reaction condition of process variable i.e. 2 wt % catalyst dose, 1:15 methanol to oil molar ratio at 65˚C for 1 h. Sr/Ti mixed metal oxide with atomic ration 4:1 showed the highest FAME conversion among all prepared catalyst manifested in Figure 6.7. This might regard to two genuine reasons, one was the fact that with increase in doping of Sr, basicity enhanced to a saturation limit (4:1 Sr/Ti) and afterwards, $SrCO_3$ started accumulating at the surface of catalyst as confirmed by XRD, SEM and FT-IR while, other one might owe to the fact that at higher alkaline earth metal doping, metal might lead for leaching from catalyst

periphery to mother liquor. Therefore, mixed metals oxide with Sr/Ti atomic ratio of 4:1 was selected as the efficient heterogeneous basic catalyst in transesterification of WCO.

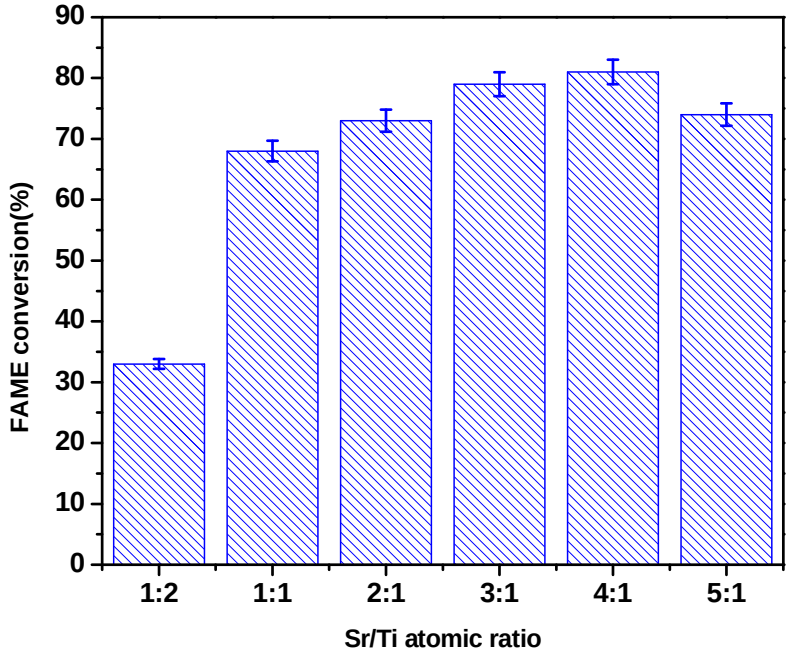

Figure 6.7 Optimization plot of Sr/Ti atomic ratio for highest FAME conversion.

6.4.2. RSM

A series of 20 experiments devised by CCD were executed to optimize the concerned process variables such as catalyst dose, methanol to oil molar ratio, reaction time in order to maximize the reaction response i.e. FAME conversion as planned in Table 6.2. Simultaneously, effect of aforementioned parameters was also monitored and observations were examined to satisfy a second-order polynomial model. Model was found to be fit as experimental and predicted responses were in close agreement. This model explored the effect of linear terms (X_1, X_2, and X_3), interaction terms (X_1X_2, X_1 X_3, and X_2 X_3) and square terms (X_1^2, X_2^2, X_3^2) on response of transesterification. Regression model equation for response of reaction was formulated

according to its dependency on process parameters which governed the fate of the process, such as catalyst dose(X_1), methanol to oil molar ratio (X_2), and reaction time (X_3). The coefficient corresponding to each process variable was computed by CCD after analyzing the experimental data deploying MINITAB 16 and further elucidated in Table 6.4. The following regression equation was generated through regression analysis of selected coded terms in transesterification for the FAME conversion as response.

$$Y = 61.3544 + 65.5539\ (X_1) + 14.7213(X_2) + 1.0543(X_3) - 51.1746(X_1^2) - 0.9219(X_2^2) - 0.0126(X_3^2) + 1.4500(X_1\ X_2) + 0.3917(X_2\ X_3) + 0.0458(X_3\ X_1) \quad (6.2)$$

The greater value of regression coefficient (>80%) substantiated the fitness of the regression second-order polynomial model (Gusain et al., 2015). In this case, R^2 value was 95% with R^2 (adj) to be 91%. Aforementioned values of R^2 validated the application of quadratic model to demonstrate the impact of process variables. P values of all the concerned variables were less than 0.05 and those were considered to be the indispensable factors in transesterification reaction. Even their quadratic effect was also found significant. The positive or negative sign of its coefficient predicted the behavior of individual process variable while the strength of its impact was measured by the magnitude of its coefficient. The positive coefficient of catalyst dose, methanol to oil molar ratio, and reaction time indicated that FAME conversion was ameliorated along with their escalation till their saturation limit. So, catalyst dose was observed to be the most dominating factor amongst all.

Table 6.4

Estimated regression coefficient of transesterification for biodiesel production using Sr-Ti mixed metal oxide as solid catalyst.

Term	Coef	SE Coef	T	P
Constant	61.3544	24.8706	-2.467	0.033
Catalyst dose	65.5539	23.6311	2.774	0.020
Methanol to oil molar ratio	14.7213	2.3631	6.230	0.000
Time	1.0543	0.3939	2.677	0.023
Catalyst dose*catalyst dose	-51.1746	8.4254	-6.074	0.000
Methanol to oil molar ratio* methanol to oil molar ratio	-0.9219	0.0843	-10.942	0.000
Time*time	-0.0126	0.0023	-5.402	0.000
Catalyst dose*methanol to oil molar ratio	1.4500	1.1308	1.282	0.229
Catalyst dose*time	0.3917	0.1885	2.078	0.064
Methanol to oil molar ratio*time	0.0458	0.0188	2.432	0.035

6.4.3. Analysis of variance

The correlation between the process parameters was established by defining the approach of quadratic model which was further substantiated by Analysis of variance (ANOVA). This quadratic model was seen to be best fit concluded through the results obtained from ANOVA and Fisher's statistical test (F-test) briefed in Table 6.5. In present optimization process, catalyst dose appeared as the most commanding variable trailed by methanol to oil molar ratio and reaction time. In fact, the catalyst dose was again noticed as most important as the highest magnitude of its square term was found

as in Table 6.4. Next, methanol to oil molar ratio followed by reaction time got the second position after catalyst dose concluded after doing careful inspection of the square terms in Table 6.5.

Table 6.5

Analysis of variance for biodiesel production using Sr-Ti mixed metals oxide as solid base catalyst

Source	**DF**	**Seq SS**	**Adj SS**	**Adj MS**	**F**	**P**
Regression	9	12919.6	12919.6	1435.51	22.45	0.000
Linear	3	1926.5	2592.1	864.03	13.51	0.001
Catalyst dose	1	5.0	492.0	492.03	7.70	0.020
methanol to oil molar	1	80.0	2481.3	2481.33	38.81	0.000
Time	1	1841.6	458.2	458.20	7.17	0.023
Square	3	10233.7	10233.7	3411.22	53.35	0.000
catalyst dose*catalyst dose	1	1376.2	2358.8	2358.80	36.89	0.000
methanol to oil molar*methanol to oil molar	1	6991.3	7654.6	7654.56	119.72	0.000
Time*Time	1	1866.1	1866.1	1866.14	29.19	0.000
Interaction	3	759.4	759.4	253.13	3.96	0.042
catalyst dose*methanol to oil molar	1	105.1	105.1	105.13	1.64	0.229
catalyst dose*Time	1	276.1	276.1	276.12	4.32	0.064
methanol to oil molar*Time	1	378.1	378.1	378.13	5.91	0.035
Residual Error	10	639.4	639.4	63.94		
Lack-of-Fit	5	621.9	621.9	124.38	35.54	0.001
Pure Error	5	17.5	17.5	3.50		
Total	19	13558.9				
R-Squared	95.28%					
Adjacent R-Squared	91.56					
Pred R-Squared	83.80					

6.4.4. Outcomes from RSM

The auto generated surface and contour plots in RSM study are defined as the graphical interpretations of interaction mode between process variables. Both surface and contour plots thoroughly informed about the effect of combination of process variables on the reaction response. A drastic increment in methyl ester conversion was noticed with both catalyst dose and methanol to oil molar ratio but soon right from certain point it started deteriorating till end limits as registered in experiments with standard orders (9, 1, 18, 2, 13) and (11, 2, 13, 4, 12) respectively. While after achieving the optimum reaction time, FAME conversion became almost stagnant with little lowering as manifested by experiments with standard order (13, 1, 19, 5, 14). The interaction effect of catalyst dose and methanol to oil molar ratio was evaluated in contour plot and surface plot of Figure 6.8(a) and Figure 6.8(b) respectively. Catalyst dose enhanced FAME conversion till 1.0 wt% beyond which methyl ester conversion got hampered due to restriction in mass transfer owing to fluid viscosity (Madhu et al., 2017). The pattern of FAME conversion faced the similar trend as in earlier case. Methyl ester conversion was recorded highest at ~10:1 methanol to oil molar ratio as illustrated in Figure 6.8(a) and Figure 6.8(b). Later, it came down because of lowering in optimal concentration of catalyst upon raising methanol molar ratio. This also troubled the separation of methyl ester from its side product as glycerol kept on getting dissolved in methanol layer forming FAME-glycerol emulsion (Banerjee et al., 2019). The course of reaction has also significant impact on FAME conversion. Within a short span of time of 30 min, considerable amount of methyl ester was produced followed by a gradual increase in conversion to the maximum level. Onwards, no appreciable methyl ester conversion occurred.

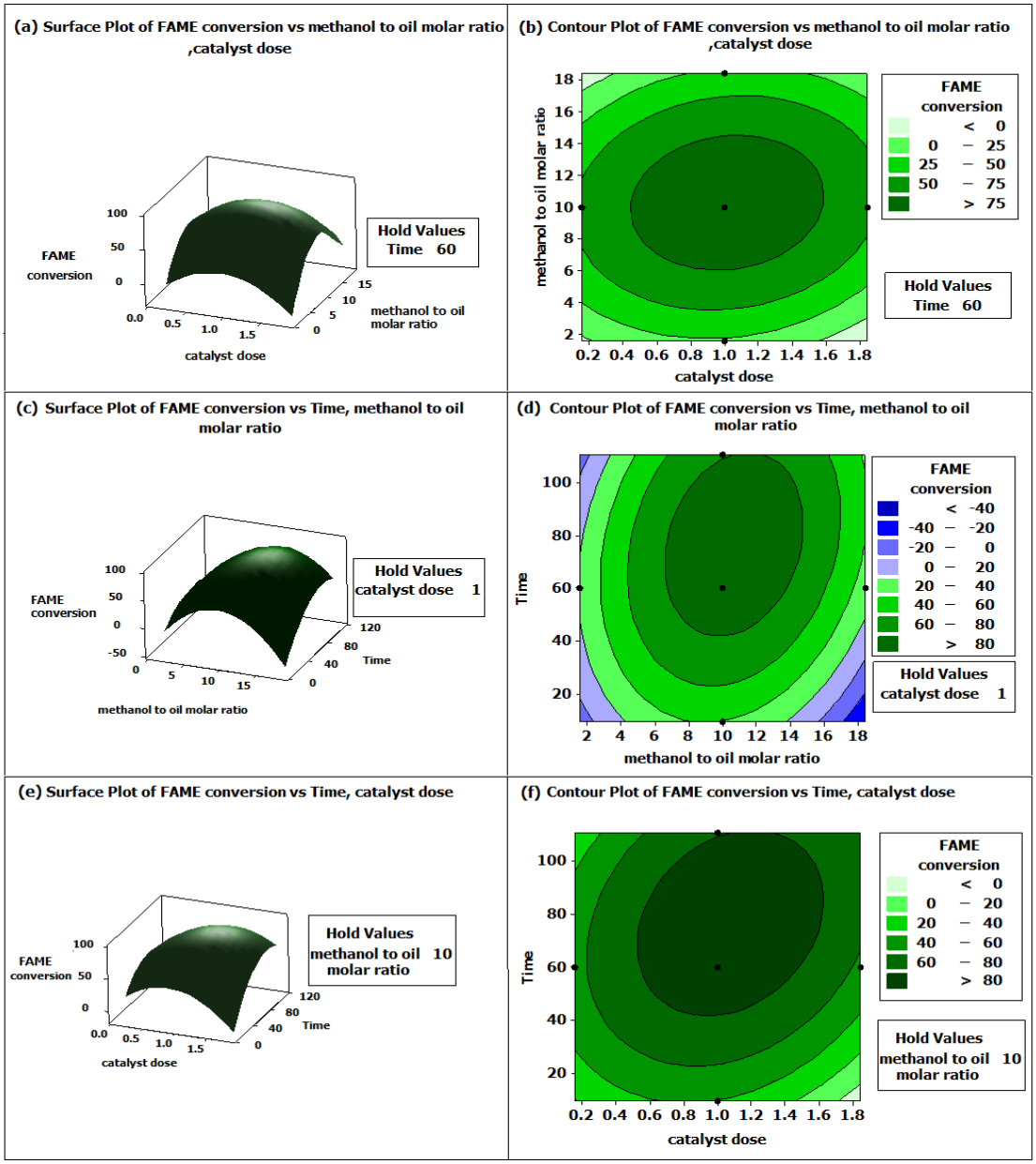

Figure 6.8 (a) Surface plot of FAME conversion vs methanol to oil molar ratio, catalyst dose (b)Contour plot of FAME conversion vs methanol to oil molar ratio, catalyst dose c) Surface plot of FAME conversion vs reaction time, methanol to oil molar ratio, (d) Contour plot of FAME conversion vs reaction time, methanol to oil molar, (e) Surface plot of FAME conversion vs reaction time, catalyst dose, (f) Contour plot of FAME conversion vs reaction time, catalyst dose.

Moreover, prolonged exposure of FAME to mother reaction mixture might lead the formation of FAME-glycerol emulsion decaying the conversion. Figure 6.8(c) and

Figure 6.8(d) revealed the interaction effect of both methanol to oil molar ratio and reaction time which predicted a Gaussian type pattern of FAME conversion for both process variables. A similar observation like above discussed was made in this case that after ~80 min and ~10:1 methanol to oil molar ratio conversion got lessened attributing to the dissolution of side product in methanol. Figure 6.8(e) and Figure 6.8(f) divulged the effect of catalyst dose and reaction time altogether on biodiesel production. Here, FAME conversion seemed to touch it apex at around ~1 wt % and~80 min clearly perceived from Figure 6.8(e) and Figure 6.8(f).

6.4.5. Validation of CCD model in RSM study

RSM concluded the ideal reaction conditions for highest probable FAME conversion as catalyst dose; 1.0wt %, methanol to oil molar ratio; 10:1, and reaction time; 77 min at 65˚C with 600rpm depicted in optimization plot (Figure 6.9). But the rationality of CCD in RSM study was assured by confirmatory experiments described in Table 6.6. It is noted that the optimum conditions of transesterification resulted from confirmatory tests were noticed very close to that of provided by RSM study. Ultimately, the highest FAME conversion of 98% was accessed at most optimum condition: 1.0 wt% catalyst dose; 10:1 methanol to oil molar ratio; 80min at 65˚C. The outcomes from confirmatory tests were quite affirmative towards CCD model used in present study. The optimized values of process variables for biodiesel production in this work unveiled the productiveness of prepared catalyst at such a low catalytic concentration alongwith moderate other reaction conditions.

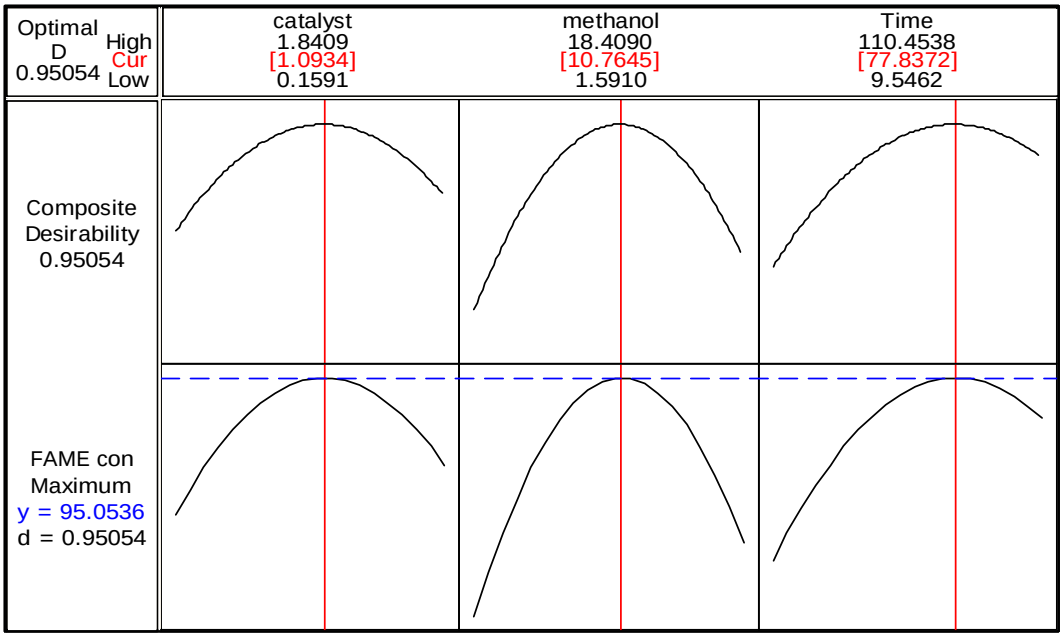

Figure 6.9 Optimization plot of process variables in transesterification reaction for biodiesel production using Sr-Ti mixed metal oxide with atomic ratio of 4:1.

Table 6.6

Confirmatory experiments for biodiesel production employing Sr-Ti mixed metals oxide as heterogeneous solid catalyst.

S.No.	Catalyst dose (wt%)	Methanol to oil molar ratio	Reaction Temperature (˚C)	Reaction time (min)	Predicted values FAME (%)	Experimental values FAME (%)
1	0.9	9	65	75	94.5	95.0
2	1.0	11	65	80	95.1	97.8
3	1.1	13	65	75	92.91	95.9

6.5. Reusability and leaching studies

The reusability of heterogeneous catalyst makes a solid catalyst more preferable over homogeneous catalyst (Sharma et al., 2009). Here, the reusability potential of catalyst was checked for the possible numbers of recycling run of transesterification to ensure its sustainability for its economical application. The prepared Sr-Ti mixed metal

oxide catalyst showed high endurance potential with 8 recycle run resulting 83% methyl ester conversion. Onwards 8th run, conversion efficiency got dropped drastically due to catalytic poisoning of surface as a result of irreversible surface passivation by organic residue and catalyst structural deformation.

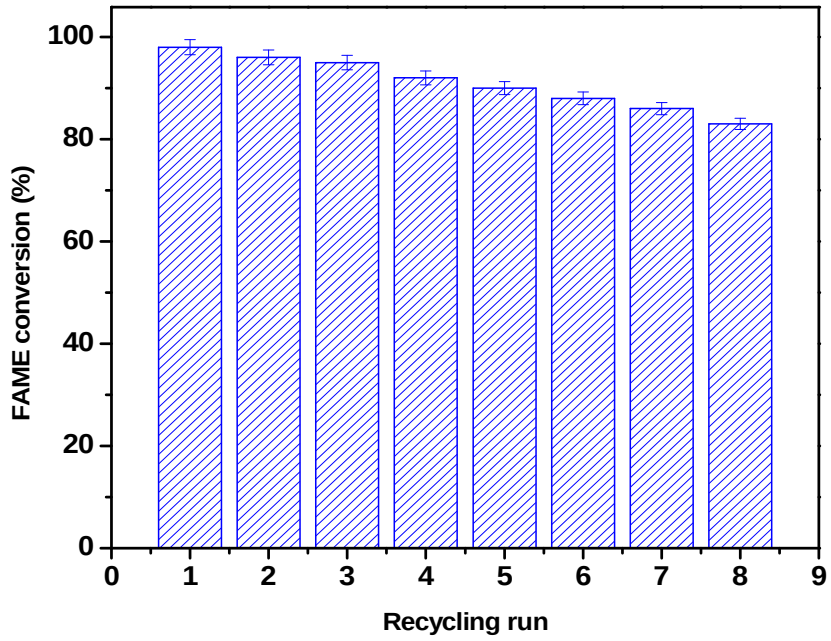

Figure 6.10 Endurance profile of catalyst efficiency over multiple recycling run.

But still the sustainability test assured the competence of catalyst for biodiesel production till the eighth cycle (Figure 6.10). Three anticipated phenomena were possibly contributed to the drastic drop in catalyst activity i.e. irreversible adsorption of organic residues of reaction mixture; leaching of active phase from catalyst into biodiesel phase or methanol system during recycling; structural modification of catalyst during regeneration process (Sahani et al., 2019). Figure 6.11 described the difference in FT-IR spectra of reused catalyst and fresh catalyst. Moreover, the concept of leaching of active phase into the reaction mixture was discarded as EDXS histogram of both fresh and spent catalyst did not manifest any peculiar difference in atomic % of

Sr/Ti. The FT-IR spectra of recycled catalyst achieved this conclusion that catalyst surface got deposited with bulkier groups extracted from triglyceride moiety during surface chemical reaction in transesterification. The conclusion drawn from FT-IR spectra has been manifested in a schematic diagram of tentative reaction mechanism (Figure 6.12).

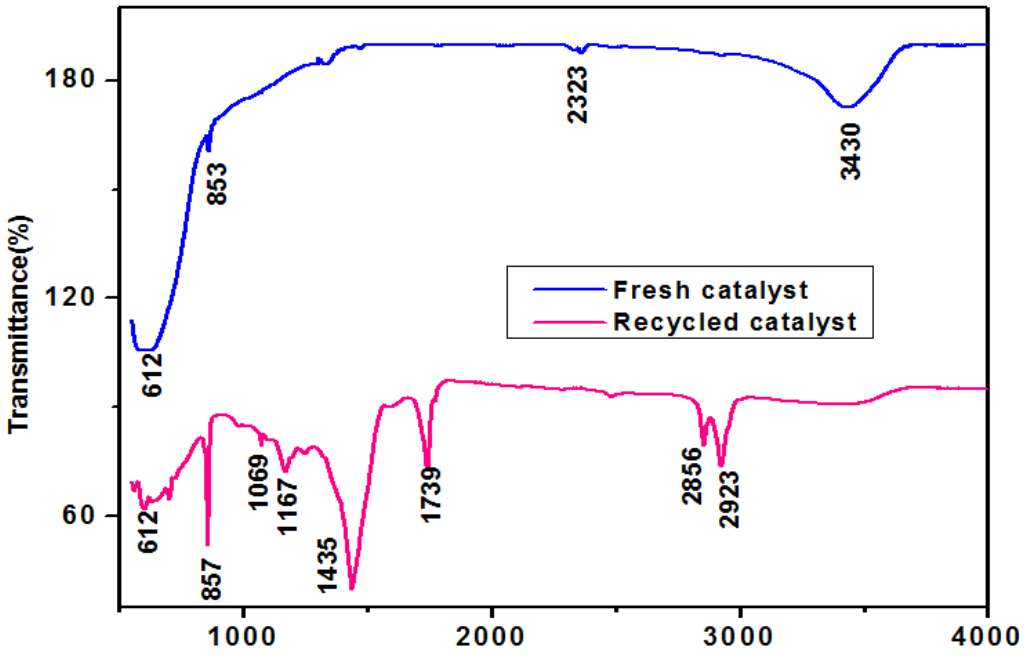

Figure 6.11 FT-IR spectra of spent catalyst before and after regeneration process.

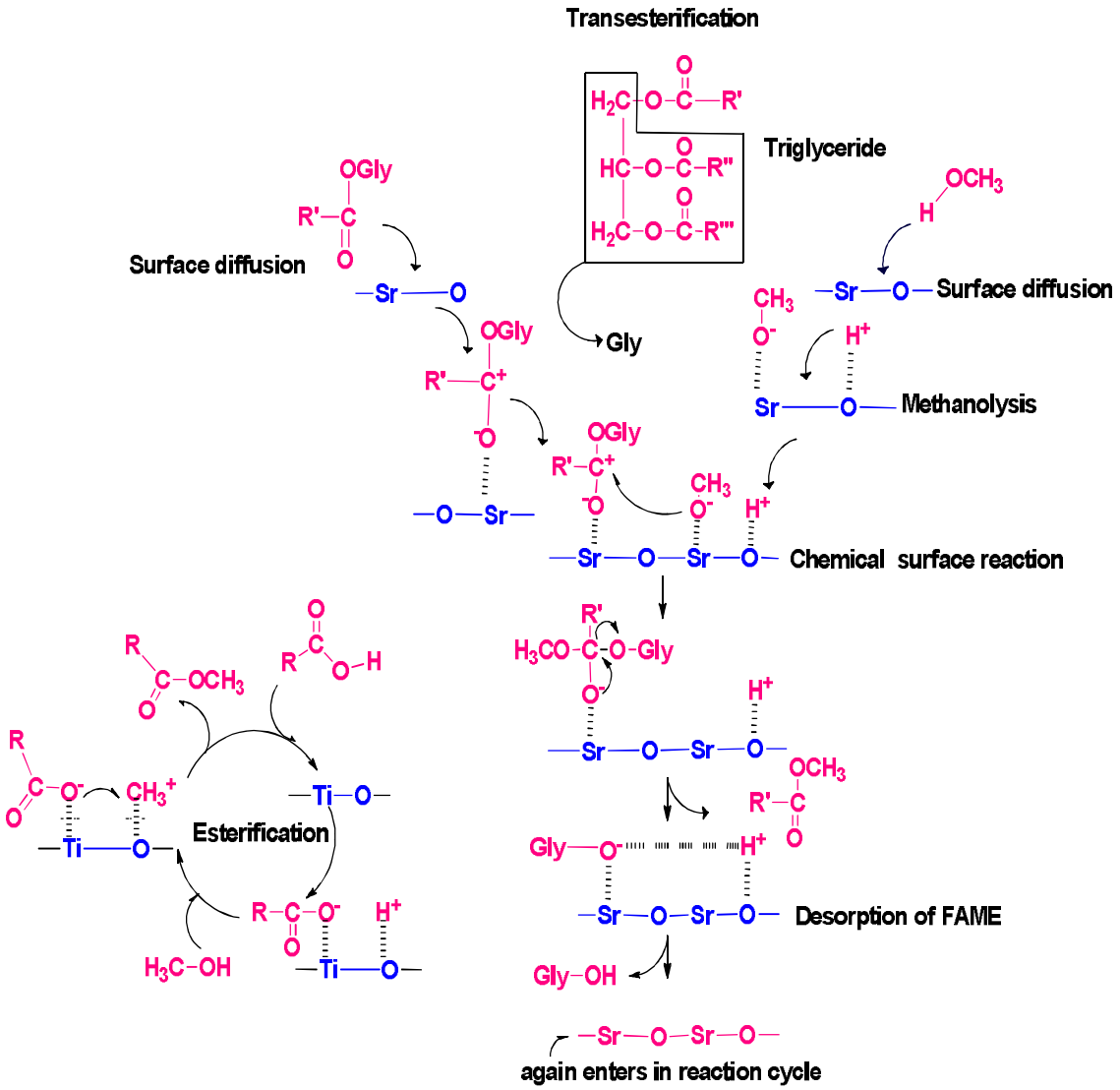

Figure 6.12 Schematic illustration of reaction mechanism followed by catalyst.

6.6. Kinetic and thermodynamic studies

The validity of presumed pseudo first order kinetics was tested by plotting the graph corresponding to –ln (1-C_{ME}) versus time at different temperature (50˚C, 55˚C, 60˚C, and 65˚C). Fortunately, the resultant plots were found decently linear displaying the high R^2 values (>95%) shown in Figure 6.13(a). This approved the predicted pseudo first order kinetics for transesterification reaction for biodiesel production. The reaction rate constant (k) was calculated to be 3.2× 10^{-2} min^{-1}, 4.0 × 10^{-2} min^{-1}, 4.4 ×

10^{-2} min^{-1}, and 5.5× 10^{-2} min^{-1} at 50˚C, 55˚C, 60˚C, and 65˚C, respectively as in Figure 6.13(a). This was inferred from this figure that temperature enhancement increased the rate of the reaction abruptly right from 50˚C to 65˚C. This affirmed the endothermic nature of transesterification process. The linear plot of Arrhenius equation in Figure 6.13(b) gave out the activation energy (E_a) value of 29.67 kJ/mol alongwith frequency factor (A) of 2.03 × 10^3 min^{-1}. The values of these two parameters were also found in close agreement with those of reported in literature (Yadav et al., 2018; Banerjee et al., 2019). The appreciably higher value of activation energy has urged the requirement of high energy to make the reaction feasible in terms of heat energy. However, the moderate value of rate constants and significantly fair value of frequency factor enabled the present Sr-Ti mixed metal oxide catalyzed transesterification reaction, an economically viable reaction. From Figure 6.13(c), values of ΔH˚ and ΔS˚ were computed to be 27.58 kJ/mol and -188.81J/mol, respectively from the linear plot of Eyring equation i.e. ln (k/T) versus 1/T. The positive value of ΔH˚ deduced the endothermic nature of transesterification reaction which meant that the external energy supplement was needed for transformation of reactants to products in between generation of activated complex (Banerjee et al., 2019), whereas the negative value of ΔS˚ value was the indication of deduction in system randomness. Ultimately, ΔG˚ values were assessed to be 88.56 kJ/mol, 89.51 kJ/mol, 90.45kJ/mol, and 91.39 kJ/mol at 50˚C, 55˚C, 60˚C and 65˚C respectively. The positive ΔG˚ values asserted the non-spontaneity of the transesterification reaction at any chosen temperature even at most optimized temperature condition (Sahani et al., 2019). Rather it declared the desirability of a catalyst to make this transesterification reaction feasible to produce biodiesel by renewing path of mechanism with relatively lower activation energy.

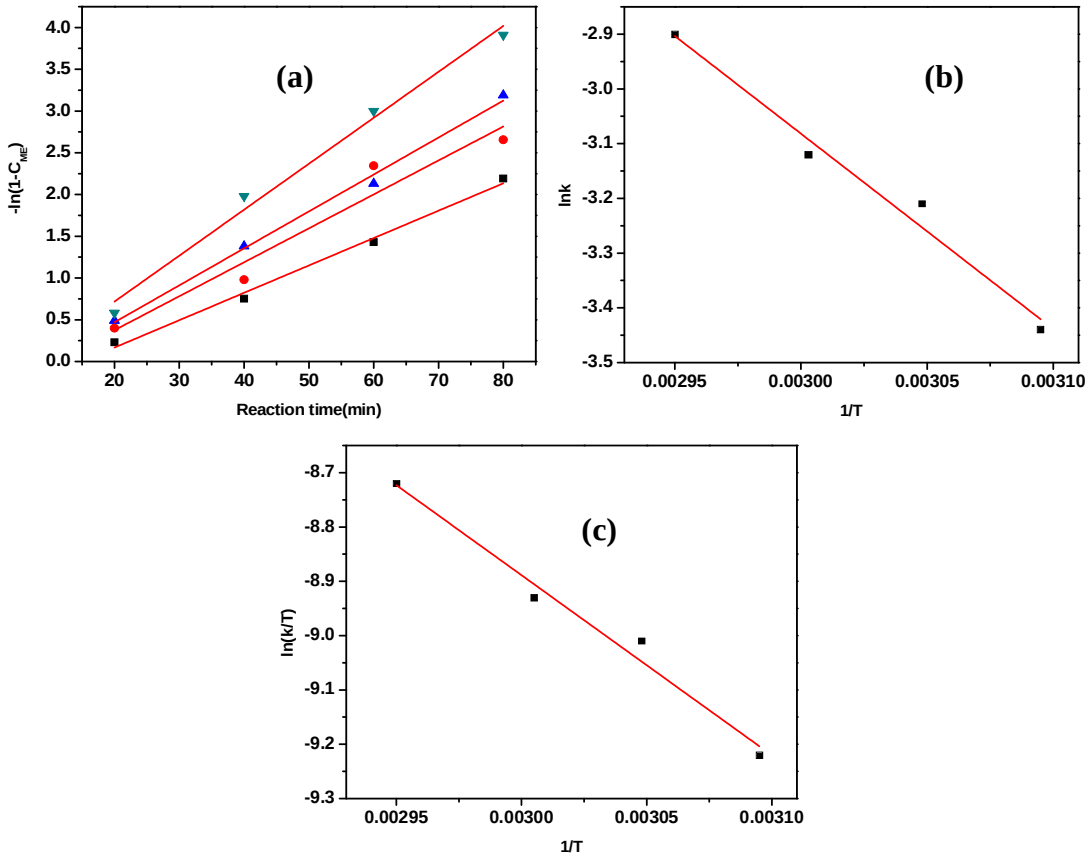

Figure 6.13 (a) $-\ln(1-C_{ME})$ versus reaction time (min) plot for pseudo-first order kinetics,(b) Arrhenius plot,(c) Eyring plot.

6.7. E-factor and TOF

The E-factor for this process of biodiesel production was 0.087 which was quite low indicating the greenness of the transesterification reaction. In current study, TOF for transesterification reaction was found as 28.56×10^{-2} s^{-1}. Roy et al. (2019) and Ranganathan et al. (2005) supported the present findings.

6.8. Methyl ester characterization

6.8.1. GC-MS

The GC-MS profile of the synthesized FAME (Figure 6.14) enlightened the presence of various types of fatty acid methyl esters. The prepared biodiesel had methyl

ester of hexadecanoic acid, 9,12-octadecadienoic acid (Z,Z), 9-octadecenoic acid methyl ester (E), octadecanoic acid, nonadecanoic acid and docosanoic acid. These above mentioned fatty acids were found to be the major fatty acid components in synthesized FAME. Nonetheless, linoleic acid appeared as the prominent constituent of biodiesel which was also corroborated by ^{1}H-NMR.

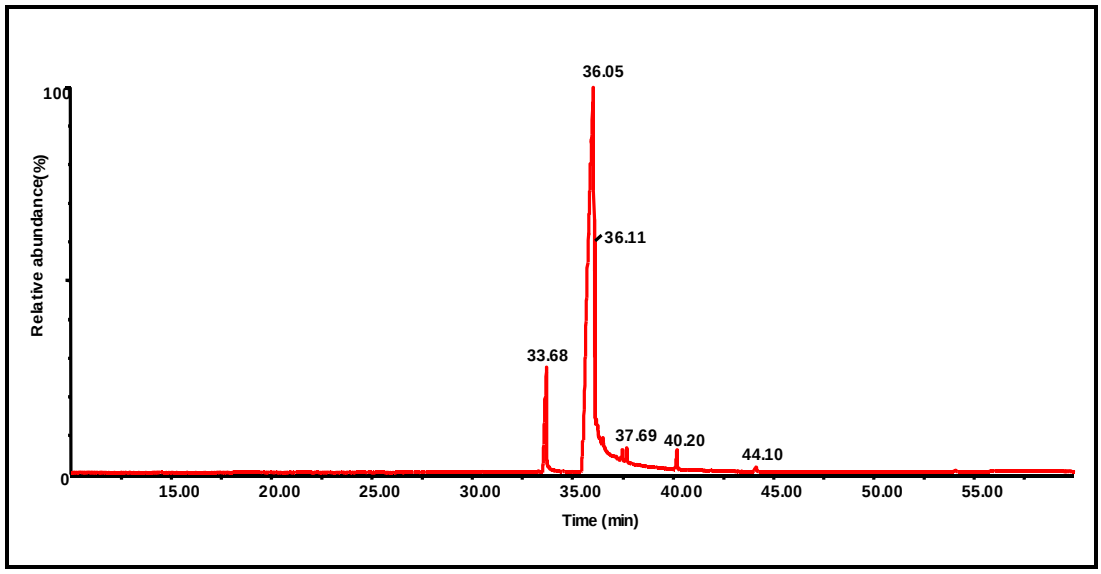

Figure 6.14 GC-MS profile which informed about the composition of synthesized FAME.

6.8.2. ^{1}H-NMR and ^{13}C-NMR

The prepared FAME was characterized by ^{1}H-NMR spectroscopy to probe its proton profile. Figure 6.15(a) illustrated NMR spectra constituting the characteristic peaks of methoxy protons at δ3.68 ppm (singlet) which authorized the methyl ester conversion during transesterification. The extent of methyl ester conversion was determined by proportionating the integration values of signals attributing to O-CH_3 and OCH_2 (triplet signal at δ 2.30 ppm was related of α-CH_2 protons of ester) (Madhu et al., 2017).

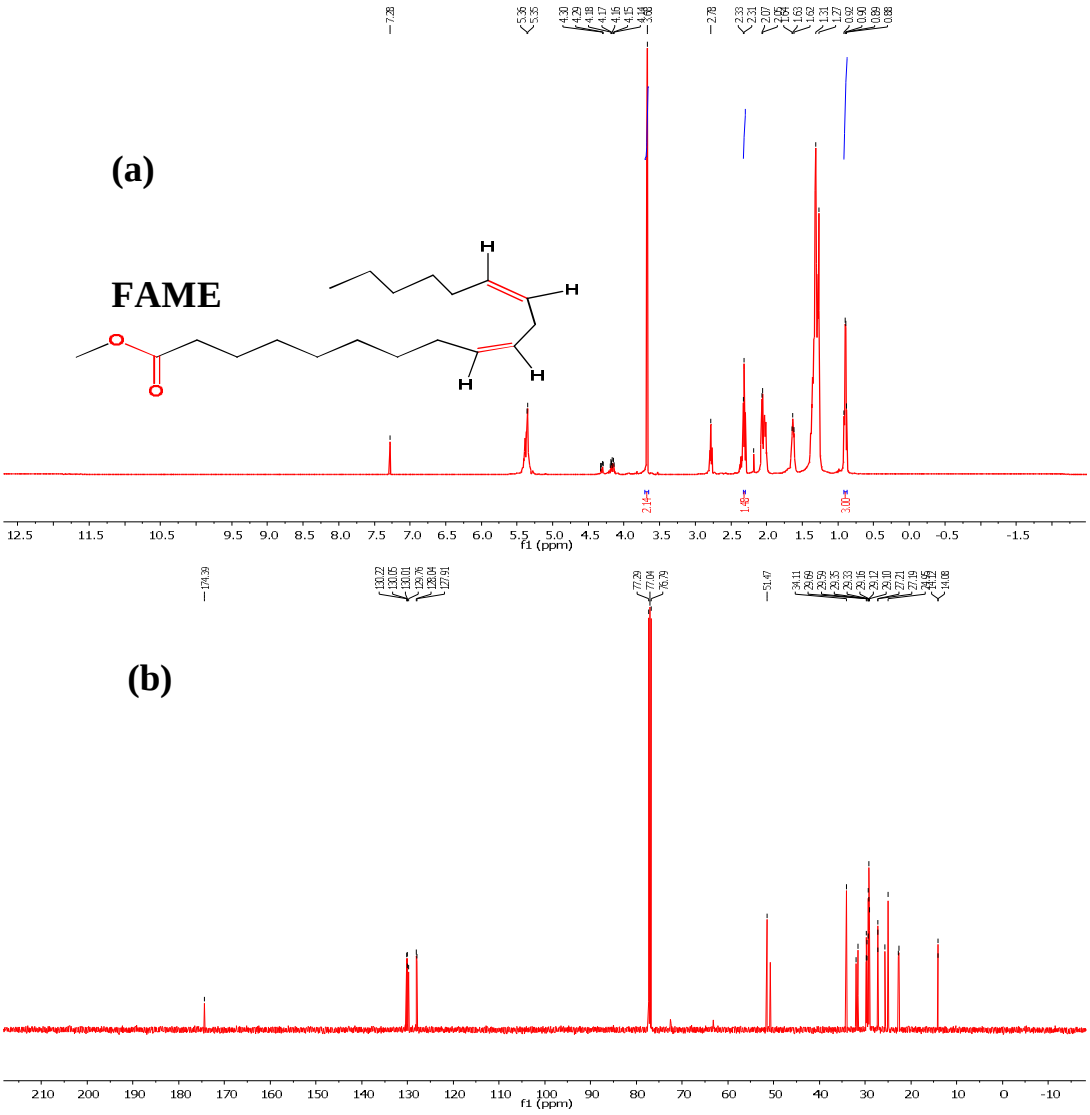

Figure 6.15. ^{1}H-NMR spectra of biodiesel produced at optimized conditions of all process parameters.

Figure 6.15(b) exemplified ^{13}C-NMR spectrum of FAME prepared form WCO. The main characteristic peak of methoxy carbon evolved at 51.69 ppm while corresponding carbonyl carbon appeared at 174.58ppm. The high intensity signals at 127.91-130.22ppm regarded to the unsaturation because of linoleic acid methyl esters comprising biodiesel also inferred from GC-MS and ^{1}H-NMR (Roy et al., 2019).

6.8.3. ATR FT-IR

The ATR FT-IR spectrum (Figure 6.16) has the most relevant peak with lowest transmittance at 1740 cm^{-1} which was associated to C=O vibration in methyl ester.

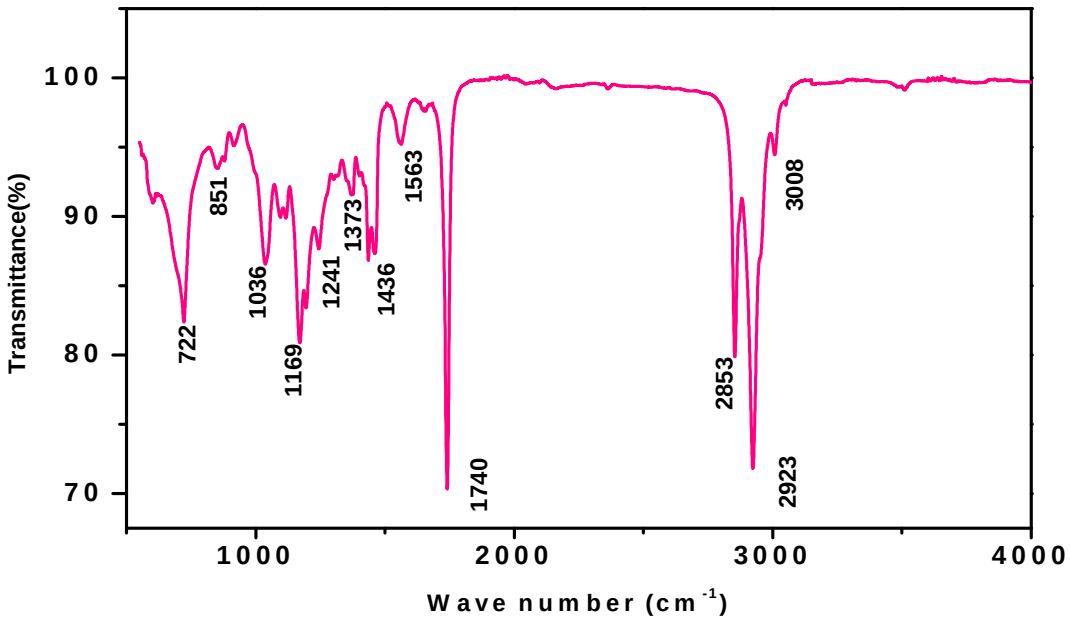

Figure 6.16 ATR FT-IR spectrum of biodiesel prepared at optimum conditions of process variables.

The peak regarding olefinic C-H stretching (-HC=CH-) was present at 3008 cm^{-1} while that of C-H of saturated carbon centre appeared at 2923 cm^{-1} alongwith the peak of C-H regarding in methoxy group at 2853 cm^{-1} (Sahani et al., 2018). The peaks with moderate intensity at 1436 cm^{-1} and 1373 cm^{-1} were attributed to asymmetric and symmetric deformations of C-H in methyl group, respectively. The peak related to -C=C- vibration was observed at 1563 cm^{-1} .The stretching and bending vibrations of -C-O-C- corresponded to the peaks at 1036 cm^{-1} , 851 cm^{-1} and 722 cm^{-1}, respectively (Madhu et al., 2017).

6.8.4. Investigation of physicochemical properties of methyl ester

The compatibility of prepared biodiesel to existing engine was insured by examining the physicochemical properties alongwith relevant fuel properties such as flash point, pour point, and kinematic viscosity. These characteristic properties were satisfactorily diagnosed within the permissible limits offered by ASTM also summarized in Table 6.7. The density of prepared FAME was very near to conventional diesel which made it quite portable. Surprisingly, the FFA value of WCO was figured out to be 1.13 mg KOH/g but soon after transesterification reaction it got lessened to 0.49 mg KOH/g. Furthermore, the kinematic viscosity of biodiesel was also reduced by transesterification of waste cooking oil drastically which enhanced the fluidity of prepared biodiesel. The most important fuel property of biodiesel i.e. flashpoint also exceeded 130˚C which is much above the diesel. It revealed the FAME as a tremendously safe fuel as its flammability was quite low even at high temperature.

Table 6.7

Physicochemical properties of biodiesel produced from WCO with ASTM standards.

Properties	**Unit**	**ASTM test method used**	**ASTM-6751 Stadards**	**FAME**
Acid value	mg KOH/g	D664	0.5max	0.49
Density (at 15˚C)	g cm^{-3}	D1298	0.878	0.880
Kinematic viscosity (at 40˚C)	mm^2/s	D445	1.9–6.0	4.1
Cetane number	-	D613	47min	48
Calorific value	MJ/Kg	D 240	39.51	40.13
Flash point	˚C	D 93	130min	138
Pour point	˚C	D 97	−15 to 10	1

6.9. Conclusions

Sr-Ti mixed metal oxide as heterogeneous base catalyst was synthesized and successfully employed in transesterification reaction for biodiesel production form waste cooking oil. Powder XRD, XPS, SEM, EDX, FT-IR, and BET surface area analysis were accomplished to determine the physicochemical properties of catalyst. The most influencing parameter i.e. basicity was calculated through Hammett indicator-benzoic acid titration method. Moreover, the highest FAME conversion was obtained by optimizing the process through RSM using CCD. The process parameters namely catalyst dose (0.5-1.5 wt%), methanol to oil molar ratio (5-15), and reaction time(30-120min) were optimized by CCD at 65˚C and 600 rpm. The above mentioned design used in RSM statistically optimized the concerned reaction parameters i.e. catalyst dose (1.09wt %), methanol to oil molar ratio (10.76:1), reaction time (77.8min) offering 96.5% methyl ester conversion. However, the confirmatory tests declared 97.9% FAME conversion using optimized reaction conditions as catalyst dose (1.0wt %), methanol to oil molar ratio (11:1), reaction time (80min). The closeness in optimized value of anticipated and confirmatory results perceived the efficiency of CCD and approved its potency as successful tool to estimate the reaction process for highest FAME conversion. A pseudo-first-order kinetic model was applied on transesterification reaction which gave out the activation energy (E_a) of 29.67kJ/mol. Furthermore, thermodynamic of the same was also explored and important thermodynamic functions (ΔH°, ΔS°, and ΔG°) were reckoned to be 27.58 kJ/mol, -188.81J/mol and 91.39kJmol^{-1} respectively. The E-factor and turn over frequency (TOF) were enumerated as 0.087 and 28×10^{-2} s^{-1}. Lastly all the critically important fuel properties of FAME produced from WCO was found to be within the permissible limit laid by ASTM standards for biodiesel. Finally, the prepared biodiesel was found suitable for its application in CI engines as a substitute of conventional fossil fuel, i.e. diesel.